(This is a sample cover image for this issue. The actual cover is not yet available at this time.)

Spectrochimica Acta Part A: Molecular and Biomolecular Spectroscopy 101 (2013) 196–203

Contents lists available at SciVerse ScienceDirect

Spectrochimica Acta Part A: Molecular and Biomolecular Spectroscopy

journal homepage: www.elsevier.com/locate/saa

Molecular structure of 4-hidroxy-3-(3-methyl-2-butenyl) acetophenone, a plant antifungal, by X-ray diffraction, DFT calculation, and NMR and FTIR spectroscopy

Oscar Enrique Piro [a], Gustavo Alberto Echeverría [a], Emilio Lizarraga [b], Elida Romano [c], César Atilio Nazareno Catalán [b], Silvia Antonia Brandán [c,*]

[a] Departamento de Física, Facultad de Ciencias Exactas, Universidad Nacional de La Plata e IFLP (CONICET, CCT-La Plata), C.C. 67, 1900 La Plata, Argentina
[b] INQUINOA–CONICET, Instituto de Química Orgánica, Facultad de Bioquímica Química y Farmacia, Universidad Nacional de Tucumán, Ayacucho 471, 4000 San Miguel de Tucumán, Argentina
[c] Cátedra de Química General, Instituto de Química Inorgánica, Facultad de Bioquímica, Química y Farmacia, Universidad Nacional de Tucumán, Ayacucho 471, 4000 San Miguel de Tucumán, Argentina

HIGHLIGHTS

- The crystal structure of the title compound has been solved by X-ray diffraction.
- The solid has two mixed and closely related conformers with unequal occupancies.
- Strong intermolecular O—H···O bonds give rise to a polymeric structure in the lattice.
- The crystallographic data affords a complete assignment of FTIR and Raman spectra.
- The observed and calculated ^{1}H and ^{13}C NMR chemical shifts are in close agreement.

GRAPHICAL ABSTRACT

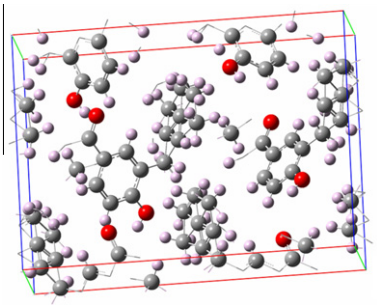

ARTICLE INFO

Article history:
Received 2 August 2012
Received in revised form 22 September 2012
Accepted 26 September 2012
Available online 5 October 2012

Keywords:
4-Hydroxy-3-(3-methyl-2-butenyl) acetophenone
Vibrational spectra
Molecular structure
Force field
DFT calculations

ABSTRACT

The molecular structure of two mixed and closely related conformers of the title compound, $C_{13}H_{16}O_2$, found in the solid with unequal occupancies has been determined by X-ray diffraction methods. The substance crystallizes in the monoclinic $Pca2_1$ space group with $a = 17.279(2)$, $b = 5.1716(7)$, $c = 12.549(2)$ Å, and $Z = 4$ molecules per unit cell. The structure was solved from 1314 reflections with $I > 2\sigma(I)$ and refined to an agreement R1-factor of 0.049. The minor conformer (34.7%) is nearly mirror-related to and extensively overlapped with the major one. The skeleton of the 4-hydroxyacetophenone molecular fragment and the prenyl group, —(CH_2)—(CH)=$C(CH_3)_2$, pendant arm attached to it are both planar and perpendicular to each other. A strong intermolecular O—H···O bond links neighboring molecules in the lattice to produce a polymeric structure. The conformational structures of the compound in the gas phase have been calculated by the DFT method and the geometrical results have been compared with the X-ray data. These data allow a complete assignment of vibration modes in the solid state FTIR and Raman spectra. The calculated ^{1}H and ^{13}C chemicals shifts are in good agreement with the corresponding experimental NMR spectra of the compound in solution.

Introduction

The 4-hydroxy-3-(3-methyl-2-butenyl) acetophenone (for short, **HMBA**) compound has mainly pharmacological interest be-

* Corresponding author. Tel.: +54 381 4247752; fax: +54 381 4248169.
E-mail address: sbrandan@fbqf.unt.edu.ar (S.A. Brandán).

1386-1425/$ - see front matter © 2012 Elsevier B.V. All rights reserved.
http://dx.doi.org/10.1016/j.saa.2012.09.086

cause this prenylated acetophenone derivative acts as an effective antifungal agent and also exhibits a moderate antibacterial activity [1]. From the chemical point of view, 4-hydroxyacetophenone derivatives prenylated at position 3 of the aromatic ring are biogenetic precursors of benzofurans and benzochromenes, two significant groups of bioactive metabolites in the plant kingdom [2]. For these reasons, the knowledge of the experimental structure of **HMBA** is important for the design and synthesis of new and better prenylated *p*-hydroxyacetophenone drugs. As part of our structural and spectroscopic studies on compounds containing different rings, such as furan, benzyl, imidazol, lactone, oxadiazole, and quinazolin rings [3–15], we have reported recently the theoretical structure and vibrational properties of **HMBA**, isolated from *Senecio nutans* Sch. Bip. (*Asteraceae*). This work was based on combined solid state infrared and Raman vibrational spectroscopy and gas phase theoretical calculation with the Density Functional Theory (DFT) method. The theoretical study showed a potential energy curve with seven stable conformers. One of them was observed in the solid state spectrum and its corresponding bands fully assigned [16]. The aim of the present paper is to report a further experimental and theoretical structural study on **HMBA** in the solid by X-ray diffraction methods and FTIR and FTRaman spectroscopies and in solution by ^{1}H and ^{13}C NMR spectroscopy. Here we disclose the X-ray crystal structure of the compound, re-analyze its solid state vibrational spectra based on this new experimental evidence, and compare this result with the optimized geometries for the seven conformers of **HMBA**, calculated previously [16]. We also discuss the corresponding NMR spectra in solution.

Experimental methods

Synthesis

Crystalline 4-hydroxy-3-(3-methyl-2-butenyl) acetophenone (**HMBA**) was obtained from aerial parts of *S. nutans*, as reported in a previous paper [16]. The substance was characterized by UV, EI-MS, ^{1}H and ^{13}C NMR, FTIR and FTRaman spectroscopy [1,16–18] and its structure was determined by single crystal X-ray diffraction method.

X-ray diffraction data

The measurements were performed at low temperature on an Oxford Xcalibur Gemini, Eos CCD diffractometer with graphite-monochromated Cu Kα (λ = 1.54178 Å) radiation. X-ray diffraction intensities were collected (ω-scans with ϑ and κ-offsets), integrated and scaled with CrysAlisPro [19] suite of programs. The unit cell parameters were obtained by least-squares refinement (based on the angular settings for all collected reflections with intensities larger than seven times the standard deviation of measurement errors) using CrysAlisPro. Data were corrected empirically for absorption employing the multi-scan method implemented in CrysAlisPro. The structure was solved by direct methods with SHELXS-97 [20] and the non-H molecular model refined by full-matrix least-squares procedure on F^2 with SHELXL-97 [21]. At this stage, a difference Fourier map showed a residual electron density which could be interpreted in terms of a minor contributing (about 34.7%) 4-hydroxy-3-(3-methyl-2-butenyl) acetophenone conformer (nearly mirror-related to the stronger diffracting molecule) which fully overlap the dominant conformer molecule except for the prenyl pendant arm. This pair of conformer molecules was refined while keeping the sum of the corresponding occupancy factors equal to one. A difference Fourier map phased on this model showed the approximated locations of several hydrogen atoms. However, they were positioned stereo-chemically and refined with the riding model. The locations of the methyl and oxydryl H-atoms were refined by treating them as rigid groups subjected to rotation around the corresponding C—C or C—O bonds such as to maximize the experimental electron density at the optimized positions. The methyl groups converged to nearly staggered conformations. Crystal data and structure refinement results are summarized in Table 1. Tables of fractional coordinates and equivalent isotropic displacement parameters of the non-H atoms, atomic anisotropic displacement parameters and hydrogen atoms positions are summarized in Tables S1, S2 and S3, respectively of the Supporting material.

NMR spectroscopy

Nuclear magnetic resonance (NMR) spectra were recorded on a Bruker 300 AVANCE spectrometer at 300 MHz for ^{1}H and 75 MHz for ^{13}C in $CDCl_3$ solutions containing 0.03 vol.% TMS as internal standard. The substance was characterized by UV, EI-MS, ^{1}H and ^{13}C NMR, FTIR and FTRaman spectroscopy [1,16–18]. GC–MS spectrum was recorded on a 5973 Hewlett–Packard selective mass detector coupled to a Hewlett Packard 6890 gas chromatograph equipped with a Perkin–Elmer Elite-5MS capillary column (5% phenyl methyl siloxane, length = 30 m, inner diameter = 0.25 mm, film thickness = 0.25 μm); ionization energy, 70 eV; carrier gas: Helium at 1.0 mL/min. UV spectra were collected on a UV–Visible 160 A Shimadzu spectrophotometer.

Computational details

In the potential energy curves reported previously for the compound, seven stable conformations (C_I, C_{II}, C_{III}, C_{IV}, C_V, C_{VI} and C_{VII}) with C_1 symmetries were obtained according to the spatial orientation of the three different substituent groups on the aromatic ring [16]. The structure of all conformers and atoms labeling can be seen in Figs. S1a and 1b of the Supporting material. The nature of all the vibration modes was established by means of the *GaussView* pro-

Table 1
Crystal data and structure refinement for 4-hydroxy-3-(3-methyl-2-butenyl) acetophenone.

Empirical formula	$C_{13}H_{16}O_2$
Formula weight	204.26
Temperature	120(2) K
Wavelength	1.54184 Å
Crystal system	Orthorhombic
Space group	$Pca2_1$
Unit cell dimensions	a = 17.279(2) Å
	b = 5.1716(7) Å
	c = 12.549(2) Å
Volume	1121.4(3) Å3
Z	4
Density (calculated)	1.210 Mg/m^3
Absorption coefficient	0.637 mm^{-1}
$F(000)$	440
Crystal size	0.19 × 0.14 × 0.04 mm^3
Crystal shape/color	Prism/colorless
ϑ-range for data collection	5.12–71.97°
Index ranges	$-16 \leqslant h \leqslant 21$, $-4 \leqslant k \leqslant 6$, $-15 \leqslant l \leqslant 15$
Reflections collected	2505
Independent reflections	1588 [R(int) = 0.0243]
Observed reflections [$I > 2\sigma(I)$]	1314
Completeness to ϑ = 71.97°	99.3%
Absorption correction	Semi-empirical from equivalents
Max. and min. transmission	1.000 and 0.729
Refinement method	Full-matrix least-squares on F^2
Data/restraints/parameters	1588/1/175
Goodness-of-fit on F^2	1.062
Final R indices[a] [$I > 2\sigma(I)$]	R_1 = 0.0490, wR_2 = 0.1190
R indices (all data)	R_1 = 0.0621, wR_2 = 0.1392
Absolute structure parameter	−0.4(5)
Largest diff. peak and hole	0.158 and −0.177 e Å^{-3}

[a] $R_1 = \Sigma||F_o| - |F_c||/\Sigma|F_o|$, $wR_2 = [\Sigma w(|F_o|^2 - |F_c|^2)^2/\Sigma w(|F_o|^2)^2]^{1/2}$.

gram [22]. The calculated chemical shielding of the ^{1}H NMR and ^{13}C NMR spectra for all conformers of **HMBA** were obtained by the GIAO method [23] at the B3LYP/6-311++G** level of theory. The calculations have been performed using the optimized geometries for this level of theory. The harmonic wavenumbers and the resulting force fields were performed following the SQMFF procedure [24] by using the MOLVIB program [25]. The natural internal coordinates for **HMBA** were reported in the Tables S1 and S2 of Ref. [14]. All calculations were performed by using the GAUSSIAN 03 program [26]. The potential energy distribution components (PED) higher than or equal to 10% are subsequently calculated with the resulting SQM. The FT-IR and Raman spectra were taken from Ref. [16].

Results and discussion

Structural analysis

Crystal and molecular structure

Fig. 1 is an ORTEP [27] plot of the dominant conformer molecule (65.3% occupancy) in the lattice. Intra-molecular bond distances and angles are in Table 2. The minor conformer (34.7%) is nearly related to the major one by a mirror reflection. The *rms* separation between homologous non-H atoms in the best least-squares structural fitting of one conformer to the other (mirror-related) one, calculated by the Kabsh's procedure [28], is 0.181 Å. As expected from an extended π-bonding structure, the skeleton of the 4-hydroxyacetophenone [(HO)C_6H_3(C═O)CH_3] molecular fragment is planar [*rms* deviation of atoms from the best least-squares plane of 0.030 Å]. The prenyl [—(CH_2)—(CH)═C(CH_3)$_2$] pendant group is also planar [*rms* value of 0.010 Å] and it is perpendicular to the above fragment to which it is attached [dihedral angle of 89.8(2)°]. The intra-molecular bond distances and angles satisfy the Organic Chemistry's rules. Particularly, the observed ring C—C bond lengths are in the 1.378(5)–1.409(5) Å range, corresponding to the expected resonant bond structure for the phenyl group. Carbonyl C═O and oxydryl C—O bond distances of 1.230(5) and 1.358(4) Å respectively agree with the double and single bond character of these links. The short C10—C11 distance of 1.306(6) Å confirms the double bond nature expected for this chemical link. The solid is further stabilized by a strong intermolecular O2—H···O1′ bond [d(O2···O1′) = 2.713 Å, <(O2—H···O1′) = 172.2°], involving the oxydryl group of a molecule as a donor and the carbonyl oxygen atom of a *c*-glide symmetry related neighboring molecule as an acceptor. This gives rise to a polymeric supra-molecular structure in the lattice (see Tables S1–S3).

Geometry optimization

The calculated bond lengths and angles for all conformers of **HMBA** reported in [16] are compared in Table 2 with the corresponding ones observed in the crystal for the dominant conformer. In general, the theoretical values for all the conformers are in agreement with one another and with the experimental values. It is to be noted that the calculation predicts that the C_I and C_{II} conformers are energetically the most stable ones contrary to the X-ray diffraction results showing that the C_{III} is the dominant conformer present in the solid state. In fact, the *rms* separation between homologous non-H atoms in the best least-squares structural fitting of the solid state main conformer to the gas phase C_{III} conformer is 0.182 Å. The difference between the experimental and theoretical results could be attributed to the effect of crystal packing forces acting on **HMBA** molecules in the lattice, perturbations not taken into account in the calculations. As mentioned above, these perturbing effects include strong O—H···O intermolecular bonds. Furthermore, the crystallization process could have selected the C_{III} rather than the C_I conformer because of the larger electric dipole moment of the former

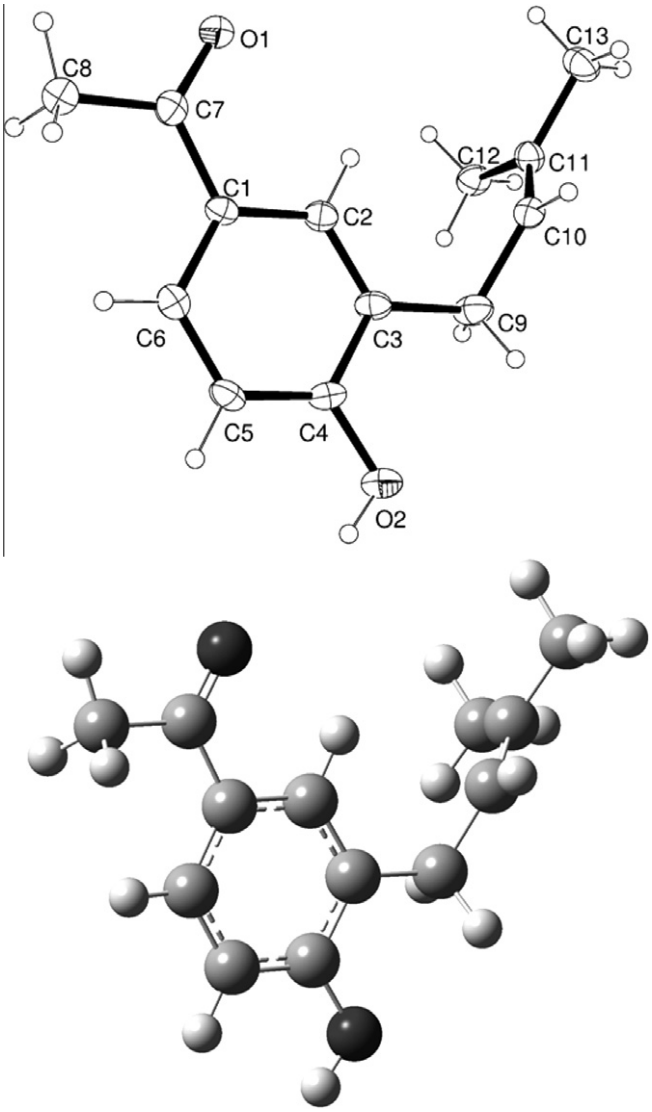

Fig. 1. Upper: view of the solid state 4-hydroxy-3-(3-methyl-2-butenyl) acetophenone main conformer showing the labeling of the non-H atoms and their displacement ellipsoids at the 30% probability level. Bottom: calculated molecular structure of the C_{III} conformer.

(4.51 D) as compared with the latter (3.52 D). Similar dependence of crystal structure stabilization upon molecular dipole moment had been observed by Ledesma et al. [29] for the anti conformer of 2-(2′-furyl)-1H-imidazole; by Sambrano et al. [30] for the M4 tautomer of 5-methylcytosine and by Brandán et al. [31] for the imino-hydroxy tautomer of 1,5-dimethylcytosine. Moreover, the C_{III} conformer showed the highest theoretical value for the $\Delta ET\pi^* \rightarrow \pi^*$ charge transfer, obtained through NBO calculations (ΔE_{Total} of 3393.78 and 3293.42 kJ/mol by using 6-31G* and 6-311++G** basis set, respectively) [14], a finding that probably justify its presence as dominant conformer in the solid. The results obtained by using the AIM analysis justify the stabilities of the C_I and C_{II} conformers, as reported previously [14].

NMR analysis

Fig. S2 shows the ^{1}H NMR spectrum for crystalline **HMBA** dissolved in $CDCl_3$, while Fig. S3 shows the corresponding ^{13}C NMR spectrum. Experimental and calculated chemical shifts for the ^{1}H and ^{13}C nuclei are compared in Tables S4 and S5 respectively. The

Table 2
Bond lengths and angles for 4-hydroxy-3-(3-methyl-2-butenyl) acetophenone.

Parameter	B3LYP/6-31G*[a]							Exp.[b]
	I	II	III	IV	V	VI	VII	
Bond lengths (Å)								
O16—C4	1.360	1.360	1.365	1.367	1.365	1.365	1.365	1.358(4)
C3—C4	1.414	1.412	1.411	1.410	1.408	1.412	1.410	1.408(5)
C3—C2	1.391	1.396	1.390	1.390	1.394	1.391	1.395	1.378(5)
C2—C1	1.404	1.403	1.406	1.406	1.405	1.405	1.403	1.409(4)
C6—C1	1.404	1.406	1.401	1.401	1.403	1.403	1.405	1.391(5)
C6—C5	1.389	1.385	1.392	1.392	1.387	1.389	1.385	1.381(5)
C4—C5	1.400	1.402	1.399	1.399	1.401	1.398	1.401	1.394(5)
C10—C1	1.491	1.491	1.492	1.492	1.492	1.492	1.492	1.474(5)
C10—C12	1.522	1.523	1.523	1.522	1.522	1.523	1.523	1.502(5)
C10—O11	1.224	1.224	1.224	1.223	1.224	1.224	1.224	1.230(5)
C3—C18	1.521	1.521	1.519	1.520	1.519	1.526	1.526	1.507(5)
C18—C21	1.514	1.514	1.513	1.513	1.513	1.506	1.507	1.532(6)
C21—C22	1.347	1.347	1.341	1.341	1.341	1.342	1.342	1.306(6)
C22—C24	1.511	1.511	1.511	1.511	1.511	1.510	1.511	1.540(7)
C22—C28	1.510	1.510	1.509	1.509	1.509	1.509	1.509	1.501(7)
RMSD[c]	**0.0170**	**0.0175**	**0.0161**	**0.0162**	**0.0162**	**0.0175**	**0.0176**	
Bond angles (°)								
O16—C4—C3	122.4	122.4	117.2	117.0	117.2	122.4	122.5	116.7(3)
O16—C4—C5	117.0	117.0	121.8	121.9	121.8	116.6	116.5	122.5(3)
C2—C3—C4	117.9	117.9	117.6	117.5	117.6	117.7	117.8	117.4(3)
C3—C2—C1	122.4	122.3	122.6	122.6	122.4	122.3	122.1	122.5(3)
C6—C1—C2	118.3	118.3	118.4	118.5	118.4	118. 6	118.6	118.8(3)
C5—C6—C1	120.6	120.7	120.3	120.3	120.4	120.5	120.6	119.7(3)
C5—C4—C3	120.6	120.6	120.9	121.1	121.0	121.0	121.0	120.7(3)
C4—C5—C6	120.2	120.1	120.1	120.1	120.1	119.9	119.9	120.8(3)
C6—C1—C10	123.3	118.6	118.4	123.1	118.4	123.2	118.5	122.6(3)
C2—C1—C10	118.3	123.1	118.4	118.4	123.2	118.3	122.9	118.6(3)
C1—C10—C12	118.8	119.0	118.8	118.8	118.9	118.8	118.9	119.3(3)
O11—C10—C1	121.1	121.0	121.0	121.0	120.9	121.1	120.9	120.8(3)
C12—C10—O11	120.1	120.1	120.2	120.2	120.2	120.1	120.1	119.3(3)
C2—C3—C18	121.0	121.0	121.8	121.8	121.8	122.6	122.4	122.9(3)
C4—C3—C18	121.1	121.1	120.6	120.7	120.6	119.6	119.8	119.7(3)
C3—C18—C21	114.0	114.0	112.3	112.5	112.4	115.0	115.0	115.2(3)
C18—C21—C22	128.4	128.4	128.5	128.2	128.5	128.2	128.2	126.7(4)
C21—C22—C28	125.0	125.0	125.1	125.3	125.1	125.1	125.1	124.7(5)
C21—C22—C24	120.5	120.5	120.4	120.4	120.4	120.5	120.5	123.0(4)
C24—C22—C28	114.4	114.4	114.5	114.2	114.5	114.4	114.4	112.2(4)
RMSD	**2.09**	**2.48**	**1.52**	**1.14**	**1.83**	**2.05**	**2.47**	

[a] This work.
[b] For the dominant 4-hydroxy-3-(3-methyl-2-butenyl) acetophenone taken from X ray.
[c] See text.

calculated chemical shifts for the H nuclei show a reasonable agreement in relation to experimental values with observed RMSD values between 0.652 and 1.105 ppm, while the chemical shifts for the carbon nuclei show higher RMSD values (4.826 and 6.363 ppm). The calculated ^{1}H chemical shifts show a good concordance for the C_I and C_{II} conformers while the calculated ^{13}C chemical shifts favors the C_{III} and C_{IV} conformers. Both results probably indicate that these conformers (C_I, C_{II}, C_{III} and C_{IV}) could be present in the solution phase. In this case, a very important observation is that the theoretical calculations do not correctly predict the chemical shift of the ^{1}H17 nucleus belonging to the hydroxy group, as observed in Table S4. This fact can be explained by the strong intermolecular H-bond observed experimentally between H17 and the carbonyl oxygen O1 atom of an acetyl moiety of a neighboring molecule.

Table S5 shows that the calculated ^{13}C chemical shifts with the GIAO method using the 6-311++G** basis set are in accordance with the experimental values. In general, the calculated shifts for the ^{13}C nuclei are higher than the corresponding experimental values.

Vibrational analysis

Based on the crystal structure results, we shall deal here only with the dominant C_{III} conformer (65.3%) of **HMBA** and its nearly-racemic counterpart (34.7%) which show occupationally disorder in the solid. Both conformers have 87 normal vibration modes, all active in the infrared and Raman spectra [14]. The experimental infrared spectrum is compared in Fig. 2 with the corresponding theoretical one for the conformer C_{III}. Table 3 shows the experimental and calculated frequencies, the SQM based on the 6-

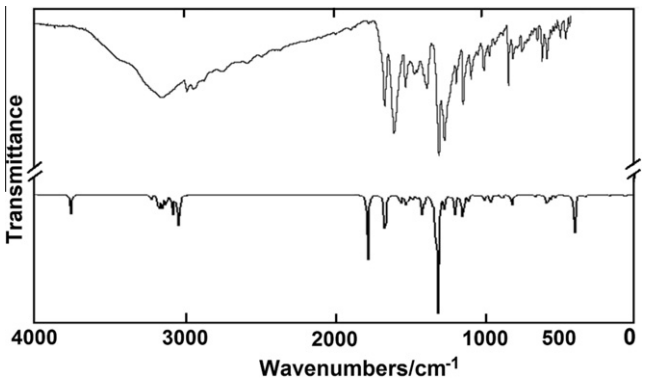

Fig. 2. Comparison between the experimental IR absorption spectrum of solid state 4-hydroxy-3-(3-methyl-2-butenyl) acetophenone reported in Ref. [14] (upper; KBr pellet) and the theoretical gas phase IR spectrum for the C_{III} conformer (bottom).

Table 3
Observed and calculated frequencies (cm^{-1}) using B3LYP method, and assignment of 4-hydroxy-3-(3-methyl-2-butenyl) acetophenone.

Experimental[e]		C_I[e]				C_{II}[e]				C_{III}[a]			
IR	Raman	SQM[b]	IR[c] int.	Raman[d]	Assignment	SQM[b]	IR[c] int.	Raman[d]	Assignment	SQM[b]	IR[c] int.	Raman[d]	Assignment
3437 w		3456	448.1	359.9	ν (O16—H17)	3462	428.5	348.4	ν (O16—H17)	3593	55.2	184.1	ν (O16—H17)
3143 s		3086	10.5	155.7	ν_s C—H	3095	4.3	120.2	ν_s C—H	3092	0.7	51.8	ν (C2—H7)
	3069 m	3073	4.4	42.1	ν (C2—H7)	3078	3.8	88.4	ν_{as} C—H	3079	11.6	106.9	ν_s C—H
		3071	5.9	50.7	ν_{as} C—H	3058	10.3	42.4	ν (C2—H7)	3037	9.3	108.7	ν_{as} CH_3
	3058 m	3037	14.8	115.9	ν_{as} CH_3 (C12)	3037	15.3	122.1	ν_{as} CH_3	3034	26.8	120.5	ν_{as} C—H
	3032 vw	3018	29.9	32.4	ν_{as} CH_3 (C28)	3017	30.6	31.3	ν_{as} CH_3	3012	33.6	33.3	ν_{as} CH_3
	3012 vw	3014	15.9	70.0	ν (C21—H23)	3014	15.2	70.3	ν (C21—H23)	3009	24.3	78.1	ν (C21—H23)
	3006 w	3000	15.4	42.9	ν_{as} CH_3 (C24)	3000	15.2	42.9	ν_{as} CH_3	2995	16.2	38.8	ν_{as} CH_3
	2990 sh	2983	11.2	50.6	ν_{as} CH_3 (C12)	2982	11.8	41.8	ν_{as} CH_3	2982	11.5	50.4	ν_{as} CH_3
2971 s	2973 m	2955	29.1	183.7	ν_{as} CH_3 (C28)	2956	28.8	183.0	ν_{as} CH_3	2948	40.8	158.2	ν_{as} CH_3
	2960 vw	2951	5.4	37.9	ν_{as} CH_3 (C24)	2951	5.3	36.7	ν_{as} CH_3	2944	13.5	101.3	ν_{as} CH_2
	2960 vw	2945	14.4	72.1	ν_{as} CH_2	2942	16.5	79.3	ν_{as} CH_2	2943	6.2	30.1	ν_{as} CH_3
2929 s	2926 m	2926	3.3	118.6	ν_s CH_3 (C12)	2925	3.7	106.8	ν_s CH_3	2926	3.5	111.9	ν_s CH_3
	2926 m	2915	45.0	408.7	ν_s CH_3 (C28)	2914	45.0	374.9	ν_s CH_3	2913	16.0	207.1	ν_s CH_2
	2926 m	2911	19.0	11.2	ν_s CH_2	2907	28.8	18.3	ν_s CH_2	2908	54.3	215.4	ν_s CH_3
2855 s	2893 sh	2906	20.6	92.2	ν_s CH_3 (C24)	2906	11.0	113.1	ν_s CH_3	2900	24.3	69.0	ν_s CH_3
1666 sh	1672 m	1703	170.7	81.1	ν (C10—O11)	1703	209.7	100.5	ν (C10—O11)	1706	142.1	61.5	ν (C10—O11)
1646 s	1646 s	1667	8.6	64.2	ν (C21—C22)	1667	7.6	66.5	ν (C21—C22)	1690	4.3	62.8	ν (C21—C22)
	1596 s	1606	157.4	146.3	ν_s C—C	1613	93.3	94.7	ν_s C—C	1602	166.0	140.0	ν_s C—C
1583 s	1583 vs	1582	40.5	40.5	ν_s C—C	1574	121.0	88.0	ν_s C—C	1589	3.1	5.8	ν_s C—C
1507 m	1506 w	1496	70.4	1.7	β C5—H8	1499	45.7	2.1	β C5—H8	1499	37.9	1.0	β C5—H8
		1461	4.4	76.4	δa CH_3 (C24)	1461	4.9	77.0	δa CH_3 (C24)	1463	2.8	61.5	δa CH_3 (C24)
		1455	13.6	1.2	δa CH_3 (C28)	1456	14.5	1.3	δa CH_3 (C28)	1455	7.8	1.2	δa CH_3 (C24)
	1452 w	1451	8.2	4.0	δa CH_3 (C28)	1451	7.5	4.1	δa CH_3 (C28)	1454	10.7	1.8	δa CH_3 (C28)
1446 m		1443	8.8	25.1	δa CH_3 (C12)	1443	9.0	23.6	δa CH_3 (C12)	1444	8.7	23.5	δa CH_3 (C12)
	1437 m	1437	0.3	31.9	δa CH_3 (C24)	1437	0.1	32.4	δa CH_3 (C24)	1437	0.5	30.0	δ CH_2 (C7)
	1437 m	1435	8.7	11.4	δa CH_3 (C12)	1436	10.3	10.5	δa CH_3 (C12)	1436	0.6	5.5	δa CH_3 (C28)
	1437 m	1431	5.6	2.1	δ CH_2	1430	3.5	1.6	δ CH_2	1434	8.9	10.0	δa CH_3 (C12)
1427 m	1428 sh	1427	24.7	5.9	ν_{as} C—C	1422	26.3	11.8	ν_{as} C—C	1423	19.9	8.4	ν_{as} C—C
1386 sh	1384 m	1389	1.8	38.0	δs CH_3 (C28)	1389	0.6	35.5	δs CH_3 (C28)	1388	0.7	27.7	δs CH_3 (C24)
	1373 sh	1379	8.1	22.0	δs CH_3 (C24)	1379	9.0	21.5	δs CH_3 (C24)	1379	7.0	19.7	δs CH_3 (C28)
1362 m		1365	22.1	3.3	ρ C21—H23	1364	2.0	4.9	ρ C21—H23	1364	18.6	2.3	ρ C21—H23
1362 m		1350	46.8	7.8	ν_{as} C—C	1349	63.5	6.7	δs CH_3 (C12)	1347	24.0	11.6	δs CH_3 (C12)
	1348 w	1347	3.9	23.7	δs CH_3 (C12)	1345	5.5	26.6	ν_{as} C—C	1340	41.6	10.3	ν_{as} C—C
	1326 w	1310	43.7	17.9	ρ CH_2	1312	13.4	2.3	β C2—H7	1318	10.9	13.5	ρ CH_2
1283 vs	1285 s	1289	96.5	31.6	ν_{as} C—C	1290	107.1	42.3	ρ CH_2	1285	15.9	2.3	β C6—H9
1283 vs		1274	165.4	19.4	ν (C4—O16)	1280	112.6	13.6	ν (C4—O16)	1264	235.4	36.8	ν (C4—O16)
	1256 sh	1267	33.2	23.0	ν (C1—C10)	1268	71.6	34.1	ν (C1—C10)	1252	170.3	15.1	wag CH_2
1245 s	1246 m	1220	81.1	18.2	wag CH_2	1223	233.1	10.0	wag CH_2	1232	101.3	16.0	β C2—H7
1245 s		1201	132.2	2.0	δ (O—H)	1207	5.1	9.3	δ (O—H)	1172	32.4	7.3	ν_{as} C—C
1167 m	1170 m	1170	13.9	4.9	ν_{as} C—C	1170	5.3	6.7	ν_{as} C—C	1163	8.2	2.4	ν (C3—C18)
	1170 m	1158	6.3	7.4	ν (C3—C18)	1153	4.8	4.4	ν (C3—C18)	1160	3.5	3.0	δ (O—H)
1121 s	1123 vw	1115	6.5	5.6	β C6—H9	1106	6.1	7.7	β C6—H9	1114	58.3	9.7	ν (C18—C21)
		1100	26.1	12.4	ν (C18—C21)	1099	26.2	9.6	ρ' CH_3 (C24)	1102	44.2	7.5	βR_1
1103 sh	1104 w	1090	1.9	0.4	ρ CH_3 (C28)	1090	1.6	0.3	ρ' CH_3 (C28)	1092	0.4	0.3	ρ' CH_3 (C28)
1068 s	1070 m	1067	4.4	16.3	β C2—H7	1069	7.4	26.1	ν_{as} C—C	1062	14.5	12.1	ν_{as} C—C
1044 sh	1031 vw	1033	1.5	1.8	ρ CH_3 (C12)	1034	1.6	1.9	ρ CH_3 (C12)	1034	0.8	2.2	ρ CH_3 (C12)
1023 w	1021 vw	1014	1.3	8.5	ρ CH_3 (C24)	1013	0.9	8.6	ν (C18—C21)	1016	3.6	3.7	ρ CH_3 (C28)
1012 sh	1010 vw	1007	4.6	1.4	ρ CH_3 (C24)	1006	4.4	1.4	ρ CH_3 (C24)	1008	3.0	1.2	ρ CH_3 (C24)
981 w	983 m	963	19.6	7.8	ρ CH_3 (C12)	979	0.6	0.6	γ C6—H9	965	28.3	6.5	γ C2—H7
962 sh		948	0.6	3.0	γ C6—H9					964	6.3	3.6	ρ' CH_3 (C12)
946 w	948 sh	945	17.3	2.4	ρ CH_3 (C28)	945	0.3	2.9	ρ CH_3 (C28)	946	0.5	2.5	ρ' CH_3 (C24)
933 sh	938 vw	941	7.5	2.1	γ C2—H7	939	36.4	7.4	ρ' CH_3 (C12)				
908 w	908 sh					913	29.6	3.8	β R_1	920	4.3	1.6	γ C6—H9

	895 m	906	30.7	3.5	γ C21—H23	907	8.3	4.7	γ C21—H23	893	0.4	1.2	τw CH_2
885 vw	882 vw	883	2.7	8.4	ν (C10—C12)	891	7.4	2.1	γ C2—H7	879	2.7	6.6	ν (C10—C12)
854 vw	855 w	848	10.1	14.4	τw CH_2	850	7.9	11.8	γ C5—H8	857	5.6	18.6	γ C21—H23
816 m	818 vw					845	21.6	3.7	τw CH_2	800	30.2	3.0	γ C5—H8
787 w	789 m	831	22.3	2.3	γ C5—H8								
776 sh	778 sh	771	7.9	3.7	ν_s C—C	776	6.1	3.7	ν_s C—C	777	16.0	13.2	ν_s C—C
744 sh	745 vw	741	3.3	16.6	ν_s C—C	742	1.9	18.1	ν_s C—C	757	1.8	2.8	ν_s C—C
727 w	731 vw	727	1.2	0.4	τ R_1	728	1.6	0.6	τ R_1	715	0.5	0.6	γ C4—O16
684 vw	687 m	681	1.7	4.6	βR_1	679	0.7	6.1	ν (C10—C12)	678	0.4	5.2	ν (C1—C10)
623 vw	625 vw	641	3.0	3.0	βR_3	640	2.3	2.5	βR_3	620	7.3	1.2	γ C10—O11
592 w	595 m	610	3.4	4.6	γ C10—O11	610	5.4	2.4	γ C10—O11	588	2.9	9.8	βR_3
	570 w					587	23.5	2.1	ρ C10—O11	564	14.4	0.4	ρ C10—O11
557 w	558 w	569	42.7	0.9	ρ C10—O11					554	24.8	0.6	ρ C22—C28
543 sh	534 vw	534	72.9	5.4	ρ C22—C28	526	68.8	4.4	ρ C22—C28				
527 w	527 w	518	3.2	1.0	τ R_3, τ R_1, γ C4—O16					518	1.7	0.2	τ R_1
512 vw	510 w	501	0.5	0.6	γ C4—O16	511	4.6	0.8	γ C4—O16				
497 vw	490 sh	490	5.6	1.5	τ OH	498	7.2	2.6	τ OH	491	8.1	1.4	β C4—O16
477 sh	472 m					479	15.7	0.4	β C4—O16				
469 vw		460	3.2	2.4	γ C21—C22					460	4.9	4.2	γ C21—C22
452 vw	457 sh					455	1.1	1.4	γ C21—C22				
441 vw	442 w	441	0.7	2.9	γ C3—C18								
435 vw	435 sh					440	0.7	2.4	γ C3—C18	439	1.3	1.2	τ R_2
407 vw	401 w	402	0.7	0.3	δ C24—C22—C28	407	2.7	1.5	δ C12—C10—C1	429	2.5	1.4	δ C12—C10—C1
	394 w	401	0.3	0.5	β C4—O16	403	0.4	0.3	δ C24—C22—C28	392	105.1	3.5	δ C24—C22—C28
	369 m	343	0.7	1.7	βR_2					361	2.4	0.6	τ OH
	336 w					336	1.7	2.5	βR_2	336	0.9	3.8	βR_2
	317 w	309	0.2	3.8	τ R_2	314	1.2	2.4	τ R_2	302	4.7	1.4	γ C3—C18
	297 m	286	1.5	0.7	β C3—C18	288	1.4	0.8	β C3—C18	294	2.3	0.4	δ C18—C21—C22
	269 m	274	2.6	1.1	τ C22—C24	274	4.0	1.2	τ C22—C24	279	1.6	1.5	τ C22—C24
	251 sh					243	3.7	3.6	δ C12—C10—C1				
	235 w	238	1.7	3.7	δ C18—C21—C22; δ C12—C10—C1					231	1.1	1.1	β C3—C18
	212 w	196	0.3	1.2	τ R_3	193	0.5	1.5	τ R_3	188	1.9	0.3	τw CH_3 (C28)
	163 vvw	171	1.4	0.9	τw CH_3 (C24)	170	1.8	1.2	τw CH_3 (C24)	171	1.2	2.5	τ R_3
		150	0.3	0.0	β C1—C10	149	0.2	0.2	β C1—C10	154	0.7	1.2	β C1—C10
	136 vvw	140	4.7	1.9	τw CH_3 (C12)	141	1.1	1.6	τw CH_3 (C12)	139	0.3	0.2	τw CH_3 (C12)
		122	0.6	0.4	τw CH_3 (C28)	122	0.5	0.4	τw CH_3 (C28)	130	0.0	0.2	τw CH_3 (C24)
		110	1.4	0.6	γ C1—C10	112	1.6	0.4	γ C1—C10	105	0.0	0.7	γ C1—C10
		81	0.5	2.9	δ CCC	82	0.4	3.2	δ CCC	68	0.9	1.3	δ (CCC)
		53	4.0	0.9	τw O11C10C	51	2.1	0.9	τwO11C1C1O	53	2.3	0.4	τw O11C1C1O
		38	0.3	2.2	τ C18—C3	38	0.8	2.0	τ C18—C3	25	0.9	4.6	τ C18—C3
		32	0.4	0.9	τ C18—C21	32	0.3	1.1	τ C18—C21	20	1.9	2.8	τ C18—C21

ν, stretching; δ, scissoring; wag, wagging; γ, out-of plane deformation; ρ, in-plane deformation or rocking; τ, torsion, τw, twisting; a, antisymmetric; s, symmetric.

[a] This work.

[b] From scaled quantum mechanics force field at B3LYP/6-31G* level.

[c] Units are km mol^{-1}.

[d] Raman activities in $Å^4$ $(amu)^{-1}$.

[e] From Ref. [14].

31G* basis set, and the assignment for **HMBA**. Note that the theoretical infrared spectrum for C_{III} conformer is in general agreement with the experimental data, especially in the 1400 and 900 cm^{-1} region where a higher intensity of the C—O stretching band at 1283 cm^{-1} is justified only by this conformer, as can be seen in Fig. 2 and Table 3. Also, the intensities of the Raman bands at 3069, 2926 and 1596 cm^{-1}, assigned to the symmetric stretching modes, as observed in Table 3, can be justified by the presence of the C_{III} conformer. Furthermore, the assignments corresponding to C_{III} is slightly different from those reported previously for the conformers C_I and C_{II} [14], as indicated in Table 3. Moreover, some observed shoulders and bands in the infrared and Raman spectra (938, 787, 534, 512, 452, 441, 251 cm^{-1}), which are not predicted in the corresponding theoretical spectra, can be attributed to the nearly-racemic counterpart of the C_{III} conformer that appears in the disordered mixture within the solid. Hence, the vibrational assignment of the experimental bands to the normal vibration modes is based on the comparison with the above assignment [16] and with the results of the calculations performed here. We considered B3LYP/6-31G* calculations because the used scale factors are defined for this basis set. The SQM force field for C_{III} structure of **HMBA** can be obtained upon request. Below, we discuss the assignment of the most important groups for the dominant conformer C_{III}.

Bands assignments

OH mode. Based on the assignments reported for molecules containing this group [6,8,10–12,16] and the theoretical calculations for the CIII conformer, the broad band observed in the IR spectrum of **HMBA** at 3437 cm^{-1} is attributed to the O—H stretching mode. The OH in-plane deformation modes for both solid state conformers were assigned at 1245 cm^{-1} while the corresponding out-of-plane deformation modes were at 497 cm^{-1}. For C_{III}, those modes are associated with the Raman bands respectively at 1170 and 731 cm^{-1}.

CH_3 modes. The calculations for the C_{III} conformer predict all vibration modes related with these groups to appear in the expected spectral regions with some differences in the frequencies of some bands, in relation to the C_I and C_{II} conformers, as observed in Table 3.

CH modes. The bands in the 3143–3012 cm^{-1} region of the IR and Raman spectra can be easily assigned to the C—H stretching modes of the C_{III} conformer as shown in Table 3. The three expected in-plane deformation modes were assigned to the IR bands at 1507, 1283 and 1245 cm^{-1} while the corresponding out-of-plane deformation modes are clearly predicted to occur between 965 and 800 cm^{-1}; for this reason, the bands observed at 981, 908 and 816 cm^{-1} in the spectra are associated with these modes (see Table 3).

CH_2 modes. Taking into account the previous assignments [16] for C_{III}, the two stretching modes are assigned to the bands observed in the spectra at 2960 and 2926 cm^{-1} while the corresponding CH_2 bending modes is assigned to the band appearing at 1437 cm^{-1}, as observed in Table 3. The wagging mode is easily assigned to the shoulder in the Raman spectrum at 1256 cm^{-1}. The IR and Raman bands at 1326 and 895 cm^{-1} are assigned respectively to the expected rocking and twisting mode, as indicated in Table 3.

Skeletal modes. For the conformer C_{III} of **HMBA**, the C=C stretching corresponding to the prenyl side chain was assigned in accordance with the values previously reported for C_I and C_{II} to the strong IR band at 1646 cm^{-1}. The remaining stretching modes were assigned as those reported in Ref. [16]. For this conformer, the shoulder and the strong band respectively at 1666 and 1646 cm^{-1} can be assigned to the C=O stretching mode in accordance to the previous assignment for C_I and C_{II} [16]. The very strong band at 1283 cm^{-1} is associated with the C—O stretching modes. As in the previous paper [16], the carbonyl stretching mode splits into two components in the infrared at 1652 and 1645 cm^{-1}. The splitting is probably due to intermolecular association based on C=O···H—O type hydrogen bonding [32]. The remaining skeletal modes were assigned as detailed in Table 3.

Conclusions

The crystal and molecular structure of 4-hydroxy-3-(3-methyl-2-butenyl) acetophenone were determined by X-ray diffraction methods. The compound was characterized by IR absorption and Raman dispersion spectroscopic techniques in the solid state and by NMR spectroscopy in solution.

The DFT calculations suggest the existence of two energetically low-laying conformations (C_I and C_{II}). Although the C_I conformation has the lowest energy in the gas phase, X-ray diffraction data indicate that the C_{III} conformation is the dominant and most stable conformation in the solid phase.

We found that the normal mode analysis, based on the DFT molecular force field for the C_{III} conformer computed with the 6-31G* basis set, provides a satisfactory description of the observed vibrational spectra. On the other hand, the observed shoulders and bands in the infrared and Raman spectra at 938, 787, 534, 512, 452, 441, 251 cm^{-1}, which are not predicted in the corresponding theoretical spectra, can be attributed to the minor quasi-enantiomeric counterpart of the dominant C_{III} conformer which occupies the same lattice site in a disordered mixture.

Acknowledgments

This work was supported by grants from CIUNT (Consejo de Investigaciones, Universidad Nacional de Tucumán), CONICET (Consejo Nacional de Investigaciones Científicas y Técnicas, R. Argentina), (PIP 1529 and PIP 0225) and ANPCyT (PME06 2804 and PICT06 2315). The authors thank Prof. Tom Sundius for his permission to use MOLVIB. O.E.P. and G.A.E. are Research Fellows of CONICET.

Appendix A. Supplementary material

Supplementary data associated with this article can be found, in the online version, at http://dx.doi.org/10.1016/j.saa.2012.09.086.

References

[1] F. Tomás-Barberán, E. Iniesta-San Martín, F. Tomás-Lorente, A. Rumbero, Phytochemistry 29 (1990) 1093–1095.
[2] P. Proksch, E. Rodriguez, Phytochemistry 22 (1983) 2335–2348.
[3] A.E. Ledesma, J. Zinczuk, A. Ben Altabef, J.J. López-González, S.A. Brandán, J. Raman Spectrosc. 40 (8) (2009) 1004–1010.
[4] C.D. Contreras, M. Montejo, J.J. López González, J. Zinczuk, S. Brandán, J. Raman Spectrosc. 42 (1) (2011) 108–116.
[5] C.D. Contreras, A.E. Ledesma, H.E. Lanús, J. Zinczuk, S.A. Brandán, Vib. Spectrosc. 57 (2011) 108–115.
[6] P. Leyton, J. Brunet, V. Silva, C. Paipa, M.V. Castillo, S.A. Brandán, Spectrochim. Acta A 88 (2012) 162–170.
[7] C.D. Contreras, A.E. Ledesma, J. Zinczuk, S.A. Brandán, Spectrochim. Acta A 79 (2011) 1710–1714.
[8] E. Romano, A.B. Raschi, A. Benavente, S.A. Brandán, Spectrochim. Acta A 84 (2011) 111–116.
[9] A.E. Ledesma, C. Contreras, J. Svoboda, A. Vektariane, S.A. Brandán, J. Mol. Struct. 967 (2010) 159–165.
[10] S.A. Brandán, F. Marquez Lopez, M. Montejo, J.J. Lopez Gonzalez, A. Ben Altabef, Spectrochim. Acta A 75 (2010) 1422–1434.
[11] L.C. Bichara, H.E. Lanús, C.G. Nieto, S.A. Brandán, J. Phys. Chem. A 114 (2010) 4997–5004.

[12] L.C. Bichara, H.E. Lanús, S.A. Brandán, J. Chem. Chem. Eng. 5 (2011) 936–945.
[13] E. Romano, N.A.J. Soria, R. Rudyk, S.A. Brandán, Mol. Simul. 37 (8) (2012) 561–566.
[14] A. Brizuela, E. Romano, A. Yurquina, S. Locatelli, S.A. Brandán, Spectrochim. Acta A 95 (2012) 399–406.
[15] E. Romano, M.V. Castillo, J.L. Pergomet, J. Zinczuk, S.A. Brandán, J. Mol. Struct. 1018 (2012) 149–155.
[16] E. Lizarraga, E. Romano, R. Rudyk, C.A.N. Catalán, S.A. Brandán, Spectrochim. Acta A 97 (2012) 399–406.
[17] F. Bohlmann, M. Grenz, Chem. Berich. 103 (1970) 90–96.
[18] M.A. Ponce, E. Gross, An. Assoc. Quim. Argent. 79 (5) (1991) 197–200.
[19] CrysAlisPro, Oxford Diffraction Ltd., Version 1.171.33.48 (Release 15-09-2009 CrysAlis171.NET).
[20] G.M. Sheldrick, SHELXS-97. Program for crystal structure resolution. Univ. of Göttingen: Göttingen, Germany, 1997. See also: G.M. Sheldrick, Acta Crystallogr. A46 (1990) 467–473.
[21] G.M. Sheldrick, SHELXL-97. Program for crystal structures analysis. Univ. of Göttingen: Göttingen, Germany, 1997. See also: G.M. Sheldrick, Acta Crystallogr. A64 (2008) 112–122.
[22] A.B. Nielsen, A.J. Holder, Gauss View 3.0, User's Reference, GAUSSIAN Inc., Pittsburgh, PA, 2000–2003.
[23] R. Ditchfield, Mol. Phys. 8 (1974) 397.
[24] P. Pulay, G. Fogarasi, F. Pang, E. Boggs, J. Am. Chem. Soc. 101 (10) (1979) 2550.
[25] T. Sundius, J. Mol. Struct. 218 (1990) 321–326.
[26] M.J. Frisch, G.W. Trucks, H.B. Schlegel, G.E. Scuseria, M.A. Robb, J.R. Cheeseman, J.A. Montgomery Jr, T. Vreven, K.N. Kudin, J.C. Burant, J.M. Millam, S.S. Iyengar, J. Tomasi, V. Barone, B. Mennucci, M. Cossi, G. Scalmani, N. Rega, G.A. Petersson, H. Nakatsuji, M. Hada, M. Ehara, K. Toyota, R. Fukuda, J. Hasegawa, M. Ishida, T. Nakajima, Y. Honda, O. Kitao, H. Nakai, M. Klene, X. Li, J.E. Knox, H.P. Hratchian, J.B. Cross, C. Adamo, J. Jaramillo, R. Gomperts, R.E. Stratmann, O. Yazyev, A.J. Austin, R. Cammi, C. Pomelli, J.W. Ochterski, P.Y. Ayala, K. Morokuma, G.A. Voth, P. Salvador, J.J. Dannenberg, V.G. Zakrzewski, S. Dapprich, A.D. Daniels, M.C. Strain, O. Farkas, D.K. Malick, A.D. Rabuck, K. Raghavachari, J.B. Foresman, J.V. Ortiz, Q. Cui, A.G. Baboul, S. Clifford, J. Cioslowski, B.B. Stefanov, G. Liu, A. Liashenko, P. Piskorz, I. Komaromi, R.L. Martin, D.J. Fox, T. Keith, M.A. Al-Laham, C.Y. Peng, A. Nanayakkara, M. Challacombe, P.M.W. Gill, B. Johnson, W. Chen, M.W. Wong, C. Gonzalez, J.A. Pople, Gaussian 03, Revision B.01, Gaussian, Inc., Pittsburgh, PA, 2003.
[27] C.K. Johnson, ORTEP-II, A Fortran Thermal-Ellipsoid Plot Program, Report ORNL-5318, Oak Ridge National Laboratory, Tennessee, USA, 1976.
[28] W. Kabsch, Acta Cryst. A32 (1976) 922–923.
[29] A.E. Ledesma, S.A. Brandán, J. Zinczuk, O.E. Piro, J.J. López González, A. Ben Altabef, J. Phys. Chem. Org. 21 (12) (2008) 1086.
[30] J.R. Sambrano, A.R. de Souza, J.J. Queralt, M. Oliva, J. Andrés, Chem. Phys. 264 (2001) 333.
[31] S.A. Brandán, G. Benzal, J.V. García-Ramos, J.C. Otero, A. Ben Altabef, Vib. Spectrosc. 46 (2008) 89–99.
[32] P.D. Vaz, P.J.A. Ribeiro-Claro, J. Raman Spectrosc. 34 (2003) 863.